AGU PUBLICATIONS

JGR

Journal of Geophysical Research: Oceans

RESEARCH ARTICLE

10.1002/2013JC009548

Special Section:
Pacific-Asian Marginal Seas

Modulation of Kuroshio transport by mesoscale eddies at the Luzon Strait entrance

Ren-Chieh Lien[1], Barry Ma[1], Yu-Hsin Cheng[2], Chong-Ru Ho[2], Bo Qiu[3], Craig M. Lee[1], and Ming-Huei Chang[2]

[1]Applied Physics Laboratory, University of Washington, Seattle, Washington, USA, [2]National Taiwan Ocean University, Keelung, Taiwan, [3]Department of Oceanography, School of Ocean and Earth Science and Technology, University of Hawaii at Manoa, Honolulu, Hawaii, USA

Key Points:
- Kuroshio transport at its origin is directly measured
- Kuroshio transport anomalies are primarily due to westward propagating eddies
- Kuroshio transport is strong in spring and weak in fall

Correspondence to:
R.-C. Lien,
lien@apl.washington.edu

Citation:
Lien, R.-C., B. Ma, Y.-H. Cheng, C.-R. Ho, B. Qiu, C. M. Lee, and M.-H. Chang (2014), Modulation of Kuroshio transport by mesoscale eddies at the Luzon Strait entrance, *J. Geophys. Res. Oceans*, *119*, 2129–2142, doi:10.1002/2013JC009548.

Received 27 OCT 2013
Accepted 9 MAR 2014
Accepted article online 14 MAR 2014
Published online 1 APR 2014

Abstract Measurements of Kuroshio Current velocity at the entrance to Luzon Strait along 18.75°N were made with an array of six moorings during June 2012 to June 2013. Strong positive relative vorticity of the order of the planetary vorticity *f* was observed on the western flank of the Kuroshio in the upper 150 m. On the eastern flank, the negative vorticity observed was about an order of magnitude smaller than *f*. Kuroshio transport near its origin is computed from direct measurements for the first time. Kuroshio transport has an annual mean of 15 Sv with a standard deviation of 3 Sv. It is modulated strongly by impinging westward propagating eddies, which are identified by an improved eddy detection method and tracked back to the interior ocean. Eight Kuroshio transport anomalies >5 Sv are identified; seven are explained by the westward propagating eddies. Cyclonic (anticyclonic) eddies decrease (increase) the zonal sea level anomaly (SLA) slope and reduce (enhance) Kuroshio transport. Large transport anomalies of >10 Sv within O(10 days) are associated with the pairs of cyclonic and anticyclonic eddies. The observed Kuroshio transport was strongly correlated with the SLA slope (correlation = 0.9). Analysis of SLA slope data at the entrance to Luzon Strait over the period 1992–2013 reveals a seasonal cycle with a positive anomaly (i.e., an enhanced Kuroshio transport) in winter and spring and a negative anomaly in summer and fall. Eddy induced vorticity near the Kuroshio has a similar seasonal cycle, suggesting that seasonal variation of the Kuroshio transport near its origin is modulated by the seasonal variation of the impinging mesoscale eddies.

1. Introduction

The Kuroshio is the primary poleward western boundary current of the western Pacific. It originates from the North Equatorial Current (NEC), passes Luzon Strait, and flows along the east coast of Taiwan, the continental slope of the East China Sea, and south of Japan [*Nitani*, 1972]. It then separates from the coast as a free inertial jet—the Kuroshio Extension [*Qiu*, 2002]. Because of its strong poleward transport of mass, heat, and salt, the Kuroshio plays an important role in large-scale ocean circulation and climate variability. As the Kuroshio flows past the South China, Philippine, and East China seas, there are many opportunities for exchange of water masses, especially in regions of strong turbulence mixing such as the Luzon Strait [*Centurioni et al*., 2004; *Jan et al*., 2008] and the lee of Green Island [*Chang et al*., 2013].

Direct measurements of Kuroshio velocity and transport are rare. During the World Ocean Circulation Experiment (WOCE), an array of moorings deployed east of Taiwan measured a Kuroshio transport of 21 Sv [*Johns et al*., 2001]. Similar transport values were obtained along the east coast of Taiwan using historical shipboard ADCP [*Liang et al*., 2003] and XBT/XCTD [*Gilson and Roemmich*, 2002] data.

The Kuroshio transport upstream of the Taiwan coast has been derived primarily with hydrographic methods. East of Luzon, various estimates of the Kuroshio transport have been reported: 20 Sv by *Sverdrup* [1942], 30 Sv by *Nitani* [1972], 14 Sv by *Qu et al*. [1998], and 27.6 Sv by *Yaremchuk and Qu* [2004]. These estimates assume a geostrophic balance and are highly sensitive to the assumed level of no motion. *Nitani* [1972] reports that the estimate of Kuroshio transport east of Luzon is reduced to 80% if the level of no motion is changed from 1200 db to 800 db, and to ~60% if the level of no motion is changed to 600 db. *Qu et al*. [1998] remark that repeated hydrographic sections are needed to minimize the effects of internal tides and eddies on the Kuroshio transport estimate. *Kontoyiannis and Watts* [1990] report that the ageostrophic component contributes to 30–60% of the Gulf Stream during periods of coalescence of cold-core rings.

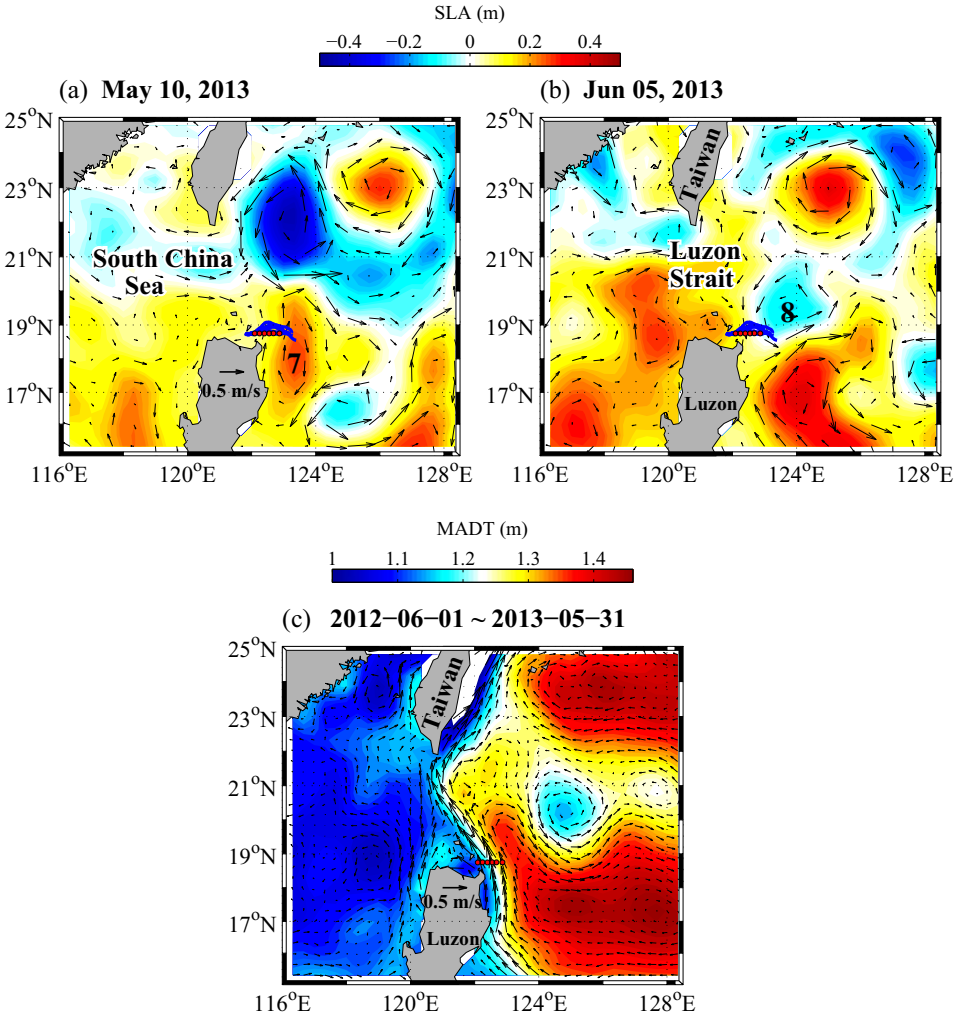

Figure 1. Positions of six moorings at the entrance to Luzon Strait (red dots), Aviso sea level anomaly (SLA) (color shading), and Aviso surface current anomaly (vectors) on (a) 10 May 2013 and (b) 5 June 2013. Velocity reference scale of 0.5 m s^{-1} is labeled in Figure 1a. Two eddies leading to Kuroshio transport anomaly events 7 and 8 are labeled in Figure 1b. Blue curves northeast of Luzon represent Seaglider tracks. Figure 1c shows the map of absolute dynamic topography (MADT) and Aviso surface current.

Johns et al. [1989], also studying the Gulf Stream, report that the velocity computed assuming geostrophic balance underestimates the current by 0.1–0.25 m s^{-1} in its core. *Toole et al*. [1990] show that the relative vorticity is significant in conserving potential vorticity in the Kuroshio, suggesting an ageostrophic balance too. Direct measurements are needed to provide a better estimate of the Kuroshio transport and to assess the assumption of geostrophy.

Seasonal variations of Kuroshio transport off the Luzon coast have been studied previously. Using a linear time-dependent Sverdrup theory and a nonlinear reduced-gravity model, *Qiu and Lukas* [1996] report that the Kuroshio across 20°N has a seasonal minimum (maximum) in fall (spring) when the NEC bifurcation is at its northernmost (southernmost) latitude. The amplitude of the seasonal variation is 5.5 Sv. Combining hydrographic data, atmospheric climatologies, and drifter data, *Yaremchuk and Qu* [2004] also report stronger (weaker) Kuroshio transport across 18.5°N in spring (fall), with an amplitude of ~3 Sv. Similar seasonal variation of Kuroshio transport was reported by *Wyrtki* [1961]. *Chang and Oey* [2012] define the Philippines-Taiwan Oscillation (PTO) as the difference between the wind stress curls averaged off the Philippines and Taiwan. During a positive PTO phase, the NEC shifts northward, eddy activity is enhanced, Kuroshio transport northeast of Taiwan increases, and westward transport into the South China Sea through Luzon Strait also increases. The later implies a weaker Kuroshio transport off Luzon following *Sheremet* [2001]. Because

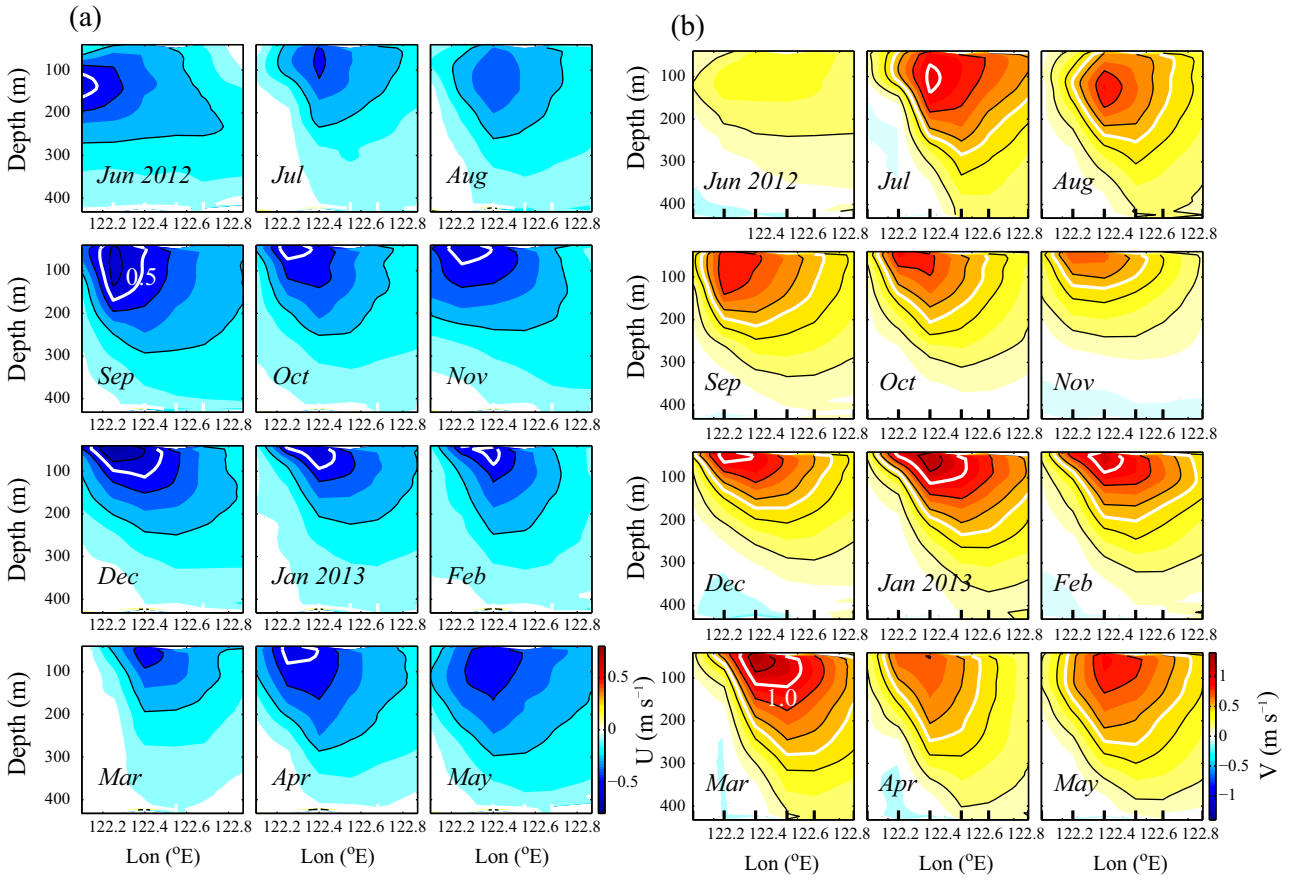

Figure 2. Monthly mean (a) zonal velocity and (b) meridional velocity measured by the moored ADCP array between June 2012 and May 2013. The black curves are constant velocity contours at a 0.2 m s^{-1} interval. The white curves are 0.5 and 1.0 m s^{-1} velocity contours. Vertical tick marks at the bottom of Figure 2b label the mooring positions.

the PTO has a clear seasonal variation, maximum in winter and minimum in summer, a seasonal variation of Kuroshio transport off Luzon is inferred from the *Chang and Oey* [2012] study.

Previous studies report that Kuroshio transport east of Taiwan is modulated strongly by the westward propagating eddies at a time scale O(100 days) [*Yang et al.*, 1999; *Johns et al.*, 2001; *Zhang et al.*, 2001; *Lee et al.*, 2013; *Chang and Oey*, 2012]. Anticylonic (cyclonic) eddies increase (decrease) Kuroshio transport. *Hsin et al.* [2013] investigate the eddy effect on the interannual variation of Kuroshio transport along the east coast of Taiwan. The relative intensity, rather than the number, of cyclonic versus anticyclonic eddies is found to be the major cause of the interannual variation of Kuroshio transport. *Vélez-Belchí et al.* [2013] demonstrate that the cyclonic eddies may also induce large Kuroshio intrusion onto East China Sea continental shelf. These eddies are generated along the North Pacific Subtropical Countercurrent (STCC) as a result of baroclinic instability between the surface eastward flowing STCC and the subsurface westward flowing NEC [*Qiu*, 1999; *Roemmich and Gilson*, 2001; *Kobashi and Kawamura*, 2002]. Except for direct mooring measurements reported by *Zhang et al.* [2001], Kuroshio transport in these studies is estimated from hydrographic surveys, sea level differences across the Kuroshio, numerical model results, or short-period shipboard surveys. Most of these studies also do not distinguish between Rossby waves and eddies.

Barron et al. [2009] report that both linear Rossby waves and eddies in the western Pacific move westward. They both contribute as westward propagating anomalies in SLA time series analyses. However, the vast majority of eddies are nonlinear, defined by the eddy Froude number $Fr = |U_{eddy}|/C_{eddy} > 1$, where $|U_{eddy}|$ is the current speed of the eddy and C_{eddy} is the eddy propagation speed [*Chelton et al.*, 2007, 2011]. Linear Rossby waves do not carry fluid effectively. Because nonlinear eddies can transport isolated water for a long distance within its inner core [*Early et al.*, 2011], their impingement and interaction could modify the Kuroshio water mass. Here we make the important distinction between linear Rossby waves and nonlinear eddies.

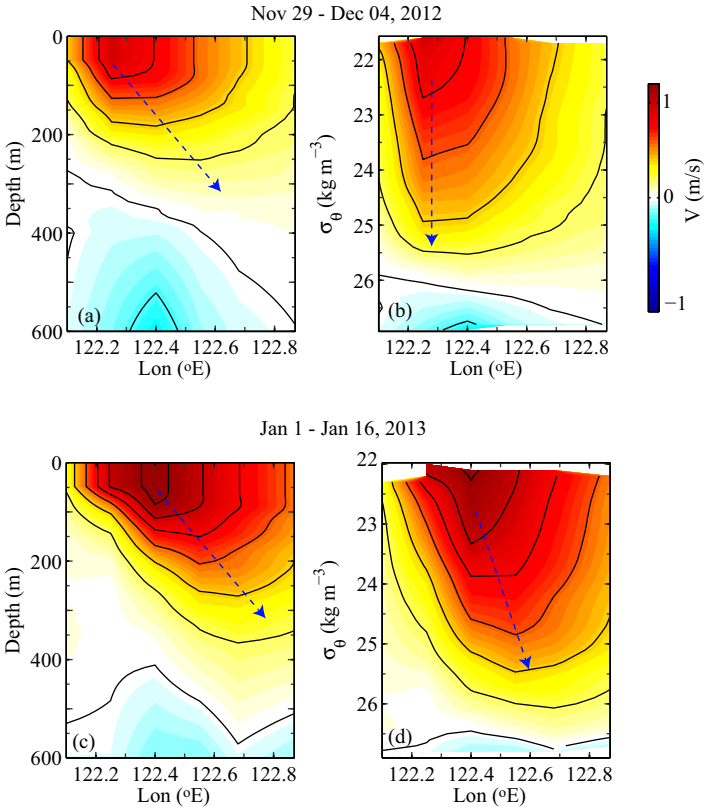

Figure 3. Kuroshio baroclinic structure in depth and density coordinates. (a and c) Kuroshio meridional velocity baroclinic structure in depth coordinates measured by the moored array averaged over 19 November to 4 December 2012 and 1 January to 16 January 2013. (b and d) The corresponding baroclinic structure in density coordinates. Blue arrows illustrate the vertical alignment of the Kuroshio axis.

Hwang et al. [2004], studying mesoscale eddies over the STCC using satellite altimetry data, report that there are more anticyclonic than cyclonic eddies. Anticyclonic (cyclonic) eddies prevail in summer (winter). These eddies often have an elliptical instead of circular shape. The effect of these eddies on the Kuroshio transport south of Luzon Strait has not been studied.

Here we analyze direct velocity measurements taken by a moored array of the Kuroshio south of Luzon Strait. Estimates of Kuroshio velocity structure and transport from the moored array are presented in section 2. A correlation of the Kuroshio transport time series with the Aviso Sea Level Anomaly (SLA) slope is presented (section 3), showing a O(10) day variability, distinctly faster than the O(100) day variability reported by previous studies of Kuroshio transport variations east of Taiwan. Methods are presented to detect, track, and analyze eddies impinging on the eastern limit of the Kuroshio. Seven of the eight observed Kuroshio transport anomalies during the mooring observation period can be explained by the westward propagating eddies. Analysis of 20 years of Aviso SLA slope data (section 4) reveals a seasonal maximum of Kuroshio transport in spring and minimum in fall. Eddy tracking analysis is applied to 20 years of Aviso data and a seasonal variation is found that is similar to the Kuroshio transport variation. A summary is given in section 5.

2. Kuroshio Velocity and Transport

2.1. Experiment and Measurements

Six moorings were deployed along 18.75°N in a zonal section between 122°E and 122.87°E, each roughly 16 km apart, spanning ~80 km at the Kuroshio entrance to Luzon Strait (Figure 1; red dots). Previous shipboard ADCP observations [*Liang et al.*, 2003], drifter observations [*Centurioni et al.*, 2004], and results from a high-resolution regional ocean model, the East Asian Seas Nowcast/Forecast System (EASNFS) of the U.S. Naval Research Laboratory [*Rhodes et al.*, 2002] were used to determine mooring positions aimed at capturing the fullest extent of the Kuroshio transport. The Kuroshio path averaged between June 2012 and May 2013 is apparent in an Aviso map of absolute dynamic topography (AMDT), showing that the major portion of Kuroshio transport is within the span of the moored array (Figure 1c).

Each mooring was equipped with one upward looking 75 kHz ADCP at 450 m nominal depth. The ADCPs took velocity measurements every 1.5 min and recorded averages every 15 min in 8 m vertical bins between 450 m and 45 m depth over the period June 2012–June 2013. The ADCP velocity measurements between the sea surface and 45 m depth were contaminated by the surface reflection of acoustic beams, but are estimated by two extrapolation methods (section 2.3.)

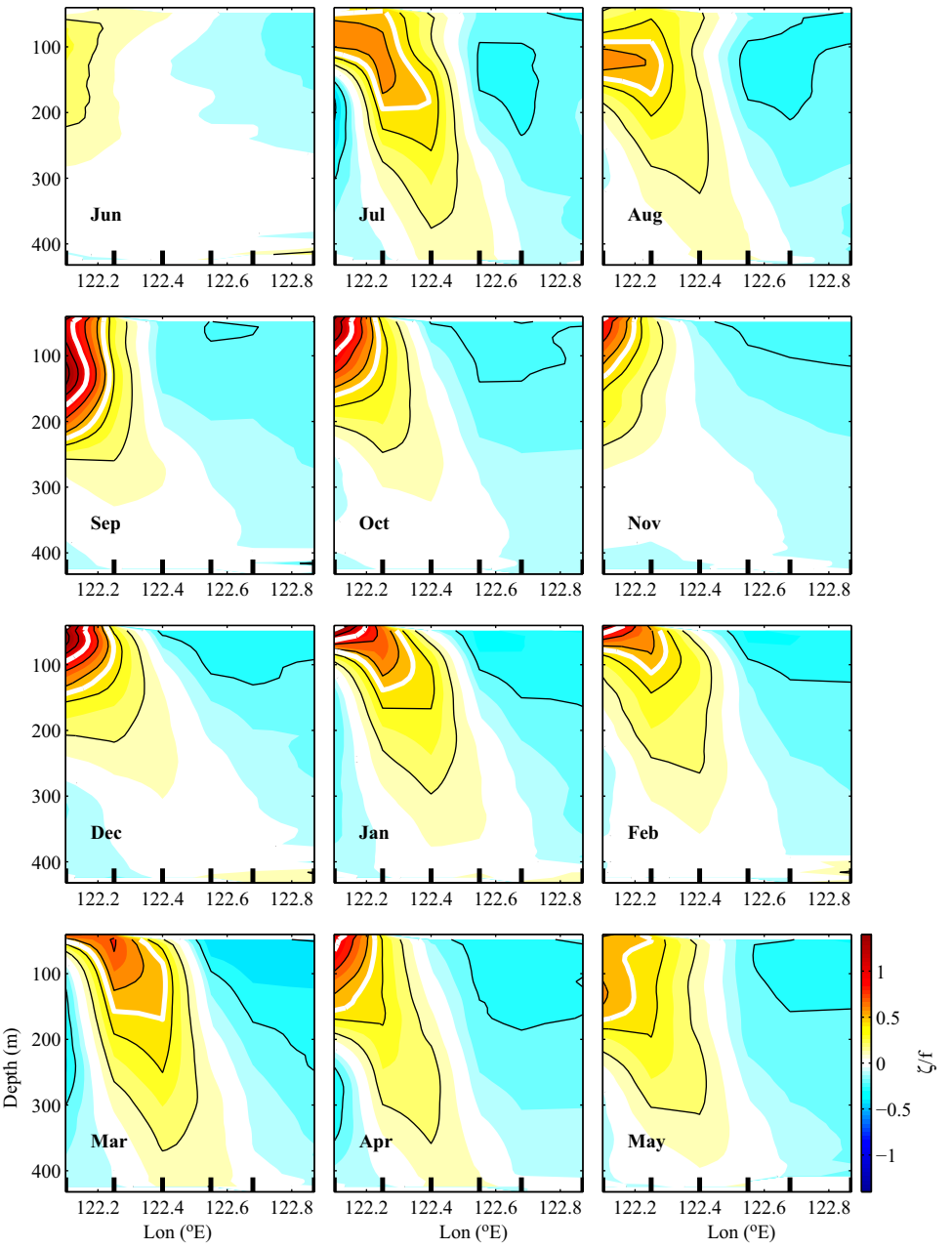

Figure 4. Monthly averaged relative vorticity ζ, normalized by the planetary vorticity f, approximated as the zonal gradient of the meridional velocity $\partial_x v$ measured by the moored ADCP array June 2012 to May 2013. The black curves are constant contours of ζ/f at 0.2 interval. The white curves are 0.5 and 1.0 ζ/f contours. Vertical ticks at the bottom of plots label the mooring positions.

Two Seagliders collected time series of high-resolution sections along the mooring line from November 2012 to May 2013 (sg124 from 3 November 2012 to 17 March 2013 and sg177 from 18 March to 31 May 2013). Seaglider is a buoyancy-driven, long-range, autonomous, underwater vehicle designed for oceanographic research [*Eriksen et al.*, 2001]. Each Seaglider was equipped with a Sea-Bird CTD, which sampled temperature and salinity every 8 s while profiling to 1000 m at roughly 0.5 m s^{-1}. The Seagliders surveyed a section between 121.8°E and 123.2°E nominally at 18.75°N along the mooring line. Strong currents associated with the Kuroshio sometimes deflected the Seaglider track from the mooring line. Fifteen transects (eight westbound, seven eastbound) were made. On average, westbound transects took 6 days and 28 dives, while eastbound transects took 12 days and 60 dives. Depth-average currents were calculated from the difference between GPS-derived surface positions at the start and end of a dive, combined with a hydrodynamic model of glider motion. Geostrophic shear normal to a section was calculated from along-section lateral density

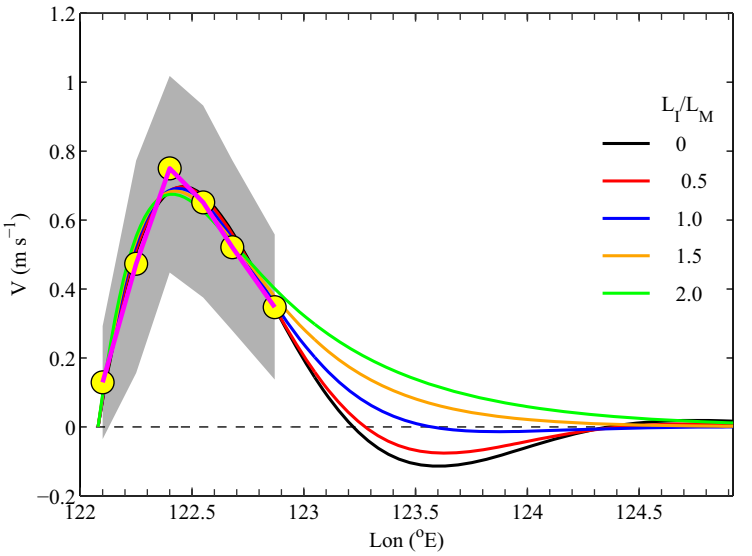

Figure 5. Comparison of the Kuroshio meridional current averaged between June 2012 and May 2013 and averaged in the upper 200 m using measurements taken by the moored array (magenta curve with yellow dots) with the theoretical Kuroshio model described by a quasigeostrophic potential vorticity equation, with different ratios of L_I/L_M, where L_I is the inertia length scale and L_M is the diffusion length scale defined in section 2.3. The shading shows the 95% confidence level of the measured Kuroshio northward current.

gradients, and turned into absolute geostrophic velocity by referencing to the glider-derived depth-average velocity.

In this analysis, Kuroshio transport is computed mainly from direct mooring measurements. The geostrophic transport estimated from Seaglider is compared with the mooring measurements and is used to evaluate the horizontal span of the Kuroshio and to identify the possible Kuroshio transport missed by the moored array (section 2.3).

2.2. Kuroshio Velocity and Vorticity

Mooring velocity data are low-pass filtered at a 10 day interval to remove tides and high-frequency fluctuations. The monthly averaged meridional current is mostly northward in the observed depth range (Figure 2). In the following analysis, we define the Kuroshio as the low-frequency meridional current being northward. One striking feature is the weak northward current, <0.5 m s^{-1}, in June 2012 (Figure 2b). As described in section 3, this is caused by the passage of a cyclonic eddy. The maximum northward current (i.e., the Kuroshio core) often exceeds 1 m s^{-1}. The axis of the Kuroshio core tilts eastward with increasing depth. Except for June 2012, the zonal current is westward within the Kuroshio, on average about 0.3−0.6 of the intensity of the northward current. The prevailing direction of the Kuroshio is $\sim$120° counterclockwise from the east. The annual mean Kuroshio axis is located at 122.43°E, varying between 122.35°E and 122.52°E. The variation of the Kuroshio axis is surprisingly small, $\pm$8 km, over an entire year.

Ratsimandresey and Pelegri [2005] demonstrate that the offshore shifting of the western boundary current axis with depth can be explained by the baroclinic structure of the density front. It is confirmed using geostrophic currents computed from an expendable bathythermograph (XBT) survey across a section of the Gulf Stream. However, western boundary currents may contain a significant ageostrophic component [*Kuehl and Sheremet*, 2009]. Therefore, a better confirmation is to use direct velocity measurements as we do here for the Kuroshio.

We compare the baroclinic structure of the Kuroshio near its origin in depth and density coordinates. Density measurements taken during each of the 15 Seaglider transects along the moored array are used to transform the mooring velocity observations, averaged during the Seaglider transects, from the depth coordinate to the density coordinate. Indeed, the offshore shifting of the Kuroshio axis is reduced significantly in the density coordinate (Figure 3), in agreement with results reported by *Ratsimandresey and Pelegri* [2005]. Our results suggest that the offshore tilt of the Kuroshio axis with depth is caused primarily by its geostrophic component. We show (section 2.3) that the ageostrophic component of the Kuroshio is small except on the western side of the Kuroshio in the upper 150 m. Note that the baroclinic structure of the Kuroshio is better presented in the density coordinate on which internal wave heaving effects can be minimized.

Toole et al. [1990] report the relative vorticity of the Kuroshio across the 18.33°N section to be important in conserving the potential vorticity. Their relative vorticity ζ was estimated using geostrophic velocity and therefore constrained by the small Rossby number (*Ro*) assumption, i.e., $\zeta < f$. We compute the relative vorticity, approximated by $\zeta \approx \partial_x v$ following *Toole et al*. [1990], using mooring velocity measurements, and therefore is not constrained by the small *Ro* assumption. Strong positive ζ exists on the western flank of the

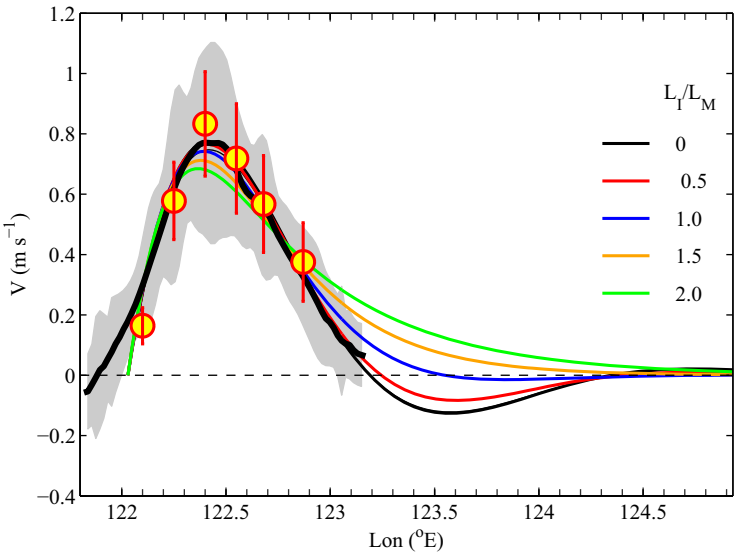

Figure 6. Comparison of the Seaglider geostrophic velocity, mooring observed velocity, and theoretical Kuroshio model. The thick black curve and shading shows the mean and 95% confidence interval of Seaglider derived geostrophic velocity averaged over the 15 Seaglider transects along the moored array and averaged over the upper 200 m. Yellow dots and vertical red lines represent the mooring observed meridional current averaged over the same period as Seaglider transects and averaged in the upper 200 m. The thinner colored curves represent the solutions of a theoretical Kuroshio model described by a quasigeostrophic potential vorticity equation with different ratios of L_I/L_M, as explained in Figure 5.

Kuroshio in the upper 150 m, often greater than 0.5*f* (Figure 4). It is sometimes greater than *f* in the upper 100 m, e.g., September, October, and December of 2012. The O(1) Rossby number suggests that the geostrophic assumption is inappropriate on the western flank of the Kuroshio. Negative ζ exists on the eastern flank of the Kuroshio, with a typical value of $-0.2f$ in the upper 150 m, suggesting that a geostrophic balance might be appropriate in the vast portion of the Kuroshio especially deeper than 150 m east of the current's axis.

2.3. Kuroshio Transport

To compute the total volume transport, the missing observations of velocity in the upper 45 m are filled using (1) linear extrapolation and (2) constant value of velocity measured at 45 m depth. The estimates of the northward transport computed from these two methods are in good agreement. We extrapolate velocity linearly from 450 m to 600 m. The maximum depth of the northward current at all six mooring positions increases from 440 m to 580 m toward the east. In this study, the Kuroshio transport is computed by integrating the northward current across the entire moored array from the surface to its maximum depth. The transports in the upper 45 m and below 450 m contribute ~20% and 13%, respectively, to the total transport.

Our mooring measurements miss a portion of the Kuroshio at its eastern limit. We use two independent methods to assess the possible missing Kuroshio transport from our mooring measurements: (1) comparing mooring observations with numerical solutions of a theoretical model of western boundary currents described by *Kuehl and Sheremet* [2009] and (2) comparing mooring observations with the geostrophic current computed from Seaglider measurements.

Following *Kuehl and Sheremet* [2009], the Kuroshio is represented by the quasigeostrophic (QG) potential vorticity advection-diffusion equation [*Kuehl and Sheremet*, 2009]

$$J\left(\psi,\ \nabla^2\psi\right)+\beta\partial_x\psi=\ A_h\nabla^4\psi$$

where ψ is the stream function, J is the Jacobian operator, $\beta=\partial_y f$, and A_h is the turbulent lateral diffusivity. This QG equation describes the balance of the nonlinear advection of the relative vorticity, the planetary vorticity, and the lateral diffusion of the relative vorticity. Note that we drop the bottom diffusion term from the *Kuehl and Sheremet* [2009] QG equation and assume that the diffusion of the Kuroshio can be approximated by the lateral diffusion. *Kuehl and Sheremet* [2009] introduce the inertia length scale $L_I=(U_\infty/\beta)^{\frac{1}{2}}$ and the lateral diffusion length scale $L_M=(A_h/\beta)^{\frac{1}{3}}$, where $U_\infty=\ -\partial_y\psi_\infty$ describes the strength of the NEC in the far field from the western boundary. The above QG equation is solved numerically using a simple centered finite difference approximation coupled with a time equilibration method also described by *Kuehl and Sheremet* [2009]. The structure of the western boundary current depends mainly on the ratio of L_I/L_M [*Sheremet et al.*, 1997].

Mooring observations averaged in the upper 200 m and over the entire measurement period are compared with numerical solutions of the above QG equation for different values of A_h and different ratios of L_I/L_M.

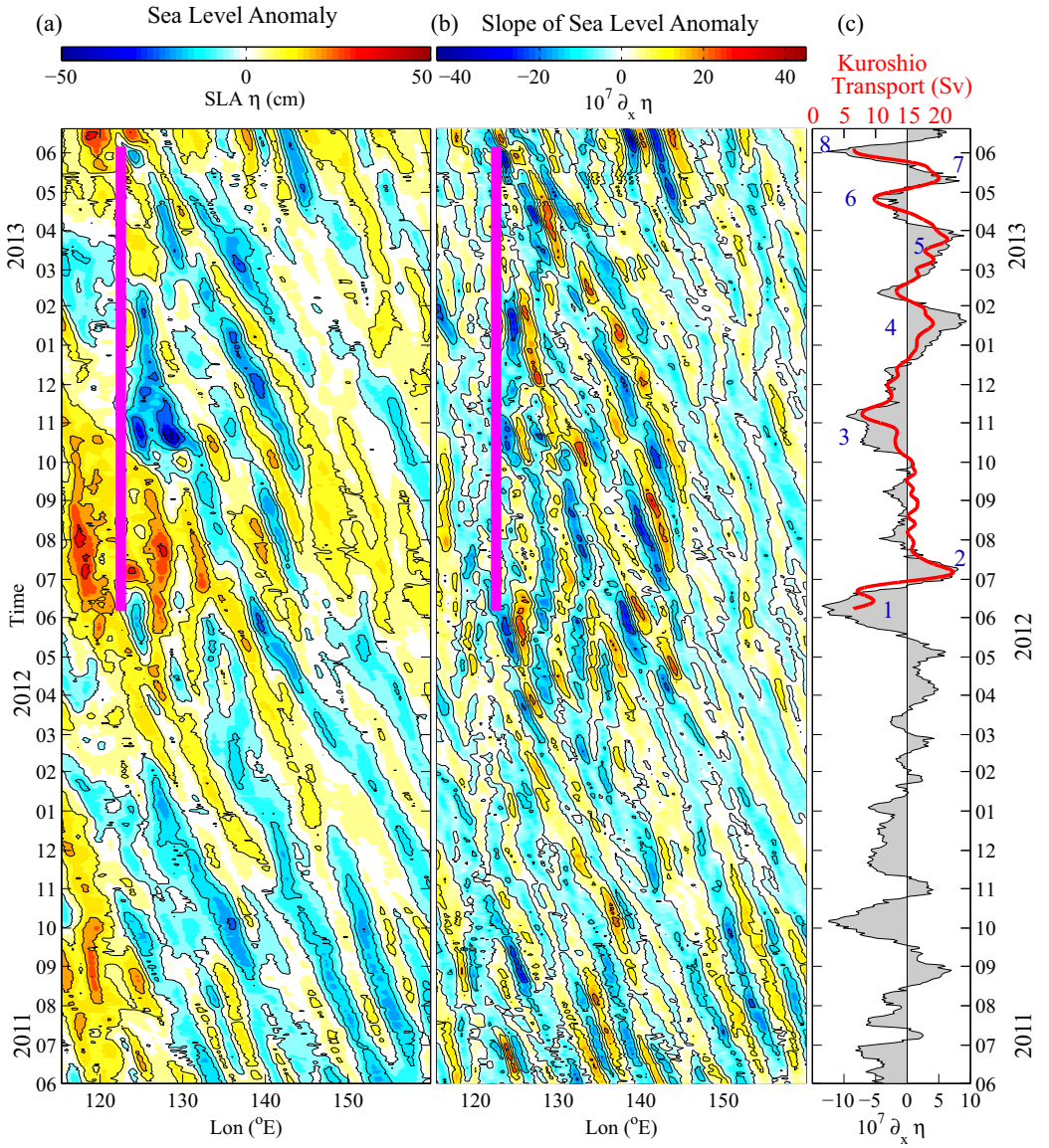

Figure 7. (a) Sea level anomaly (SLA) and (b) its zonal gradient along 18°45′N. The magenta vertical line indicates the longitude and observation period of the ADCP moored array. (c) Zonal gradient of the SLA across the moored array between 122°E and 123°E (gray shading), and the Kuroshio transport measured by the moored ADCP array (red curve). Eight events with a transport anomaly exceeding 5 Sv are labeled in Figure 7c.

Model solutions with $A_h = 800$ m^2 s^{-1} provide the best estimate of the Kuroshio axis location. Profiles of numerical solutions are fitted to the Kuroshio profile observed by the moored array (Figure 5). The solution for $L_I/L_M = 0$ reproduces the *Munk* [1950] model result, a balance between planetary vorticity and lateral diffusion. On the western flank of the Kuroshio, solutions for different values of L_I/L_M do not differ significantly. On the eastern flank of the Kuroshio, solutions for $L_I/L_M > 1$ have a long exponential tail, whereas a recirculation is present in solutions for $L_I/L_M < 1$. Previous observations [e.g., *Zhang et al.*, 2001; *Liang et al.*, 2003] and our Seaglider observations suggest that the Kuroshio has a width of 100−150 km. Solutions for $L_I/L_M > 1$ have a long exponential tail with a Kuroshio width greater than 200 km and cannot be a proper representation for the Kuroshio. Compared with solutions for $L_I/L_M = 0$, 0.5, and 1.0, mooring measurements miss 9%, 14%, and 20% of the Kuroshio transport, respectively.

Seaglider measurements cover a zonal section wider than the moored array and therefore provide a better estimate of the spatial extent of the geostrophic component of the Kuroshio. Individual sections of the

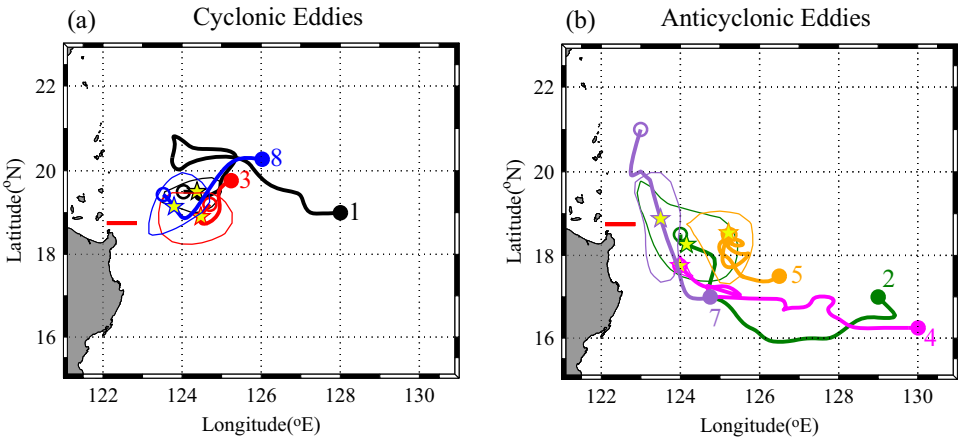

Figure 8. (a) Three cyclonic eddies and (b) four anticyclonic eddies between June 2012 and June 2013. Eddies are labeled corresponding to the anomalous events in Kuroshio transport from Figure 7c. Horizontal red line marks the mooring array position. Color lines show eddy tracks. Dots and circles represent the beginning and end of eddy tracks, respectively. Yellow stars mark positions of eddies when SLA slopes between 122°E and 123°E are the largest corresponding to the anomalous events of Kuroshio transport and the large closed color loops represent the outer boundary of eddies, defined by the boundary of maximum eddy current speed.

geostrophic current computed from Seaglider measurements might suffer from the spatial-temporal aliasing problems and therefore contain strong spatial variability. Averaged over all 15 sections, the geostrophic current from Seaglider measurements, averaged in the upper 200 m, agrees very well with that from the mooring measurements over the zonal span of the moored array (Figure 6) and suggests that mooring measurements miss 9% of the Kuroshio transport on the eastern flank of the Kuroshio. Compared to model results from the QG equation, the solution for $L_I/L_M = 0.5$ agrees the best with the geostrophic current estimated from Seaglider measurements.

On the western limit of the Kuroshio, the current may not be in geostrophic balance because of the large Rossby number and the close proximity to land. Therefore, on the western limit of the Kuroshio the geostrophic current computed by Seaglider measurements might not be representative for the Kuroshio. Combining both comparative analyses, we conclude that our mooring measurements miss less than 15% of the annual mean of the total Kuroshio transport.

To estimate the temporal variation of the missing Kuroshio transport in our mooring measurements, we linearly extrapolate monthly averaged mooring velocity measurements and define the Kuroshio boundaries where the northward current vanishes. The missing northward Kuroshio transport varies from 26% in July 2012 to 4% in November 2012, with a mean of 14% and a standard deviation of 6%. Because of the abundance of eddies east of the Kuroshio, it is a nontrivial task to define Kuroshio's boundary at time scales shorter than O(month). In the following analysis, the Kuroshio transport is referred to that computed directly from mooring measurements, without correcting for the possible missing transport on the eastern and western limits.

The annual average northward transport of the Kuroshio is 15 Sv with a standard deviation of 3 Sv (Figure 7c; red curve). This annual mean transport is close to that estimated by *Qu et al*. [1998], but significantly smaller than that estimated by *Nitani* [1972] and *Yaremchuk and Qu* [2004]. Most significantly, rapid changes of Kuroshio transport greater than 10 Sv were observed. For example, between 24 June and 4 July 2012, the Kuroshio transport increased from 7 Sv to 22 Sv. Similar transport variations of greater than 10 Sv on O(10 days) time scales were detected during May and June 2013, which is much faster than the O(100) day variations observed by *Zhang et al*. [2001] and *Lee et al*. [2013].

We fit the observed velocity averaged in the upper 200 m to the analytical form of the *Munk* [1950] solution, equivalent to the QG solution for $L_I/L_M = 0$, and determine the Kuroshio maximum current axis. Note that the Munk solution has a similar shape to that of the QG solution for $L_I/L_M = 0.5$, which shows the best agreement with our observations (Figure 5). The position of the Kuroshio axis in the upper 200 m varies only ± 8 km about 122.43°E. Therefore, we believe that the observed rapid changes in transport are not likely due to

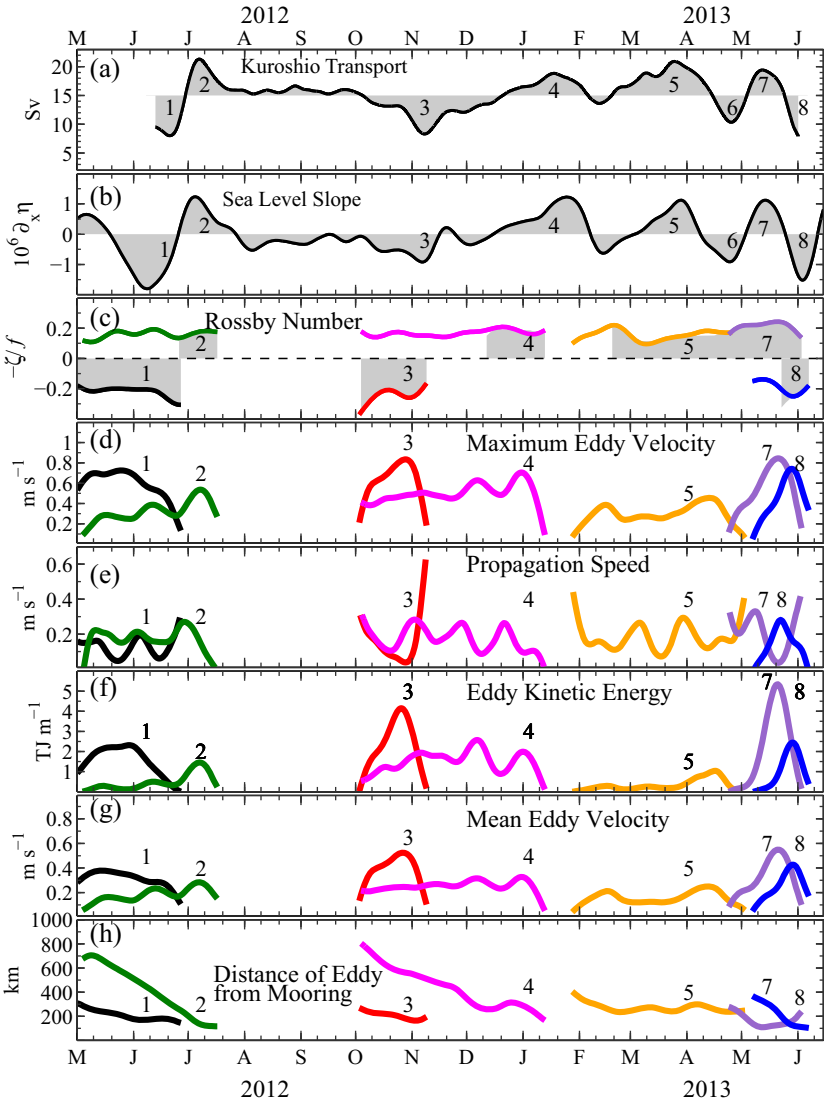

Figure 9. Time series of (a) observed Kuroshio transport computed from mooring measurements south of Luzon Strait (black curve) and (b) SLA slope between 122°E and 123°E across the mooring array south of Luzon Strait. Time series of eddy properties impinging within 250 km from the mooring south of Luzon Strait: (c) minus Rossby number, (d) maximum eddy current speed, (e) eddy propagation speed, (f) area integrated eddy kinetic energy, (g) area averaged eddy current speed, and (h) distance between the eddy center and the eastern Kuroshio boundary, ~18.75°N 123°E. Kuroshio transport anomaly events and corresponding SLA slope events and eddies are labeled. All variables have been low-pass filtered at a 10 day time scale.

the meandering of the Kuroshio off the moored array. In fact, the observed rapid transport anomaly is due to the modulation by mesoscale eddies.

3. Mesoscale Eddy Effects on Kuroshio Transport

Westward propagation of sea level anomalies (SLAs) in the western Pacific is observed by satellite altimeters [e.g., *Roemmich and Gilson*, 2001; *Chelton et al.*, 2011]. The SLA and the zonal SLA slope at the latitude of our mooring array (18.75°N) show clear westward propagations with a speed of ~0.14 m s^{-1} (Figures 7a and 7b). The altimeter products were produced by Ssalto/Duacs and distributed by Aviso, with support from CNES (http://www.aviso.oceanobs.com/duacs/). The westward propagations stall east of 123°E, i.e., east of the Kuroshio eastern limit. West of the Kuroshio (122°E), in Luzon Strait, the SLAs vary less than those on the eastern side and typically at a longer time scale. For example, a low SLA persists west of 122°E during January to March 2013.

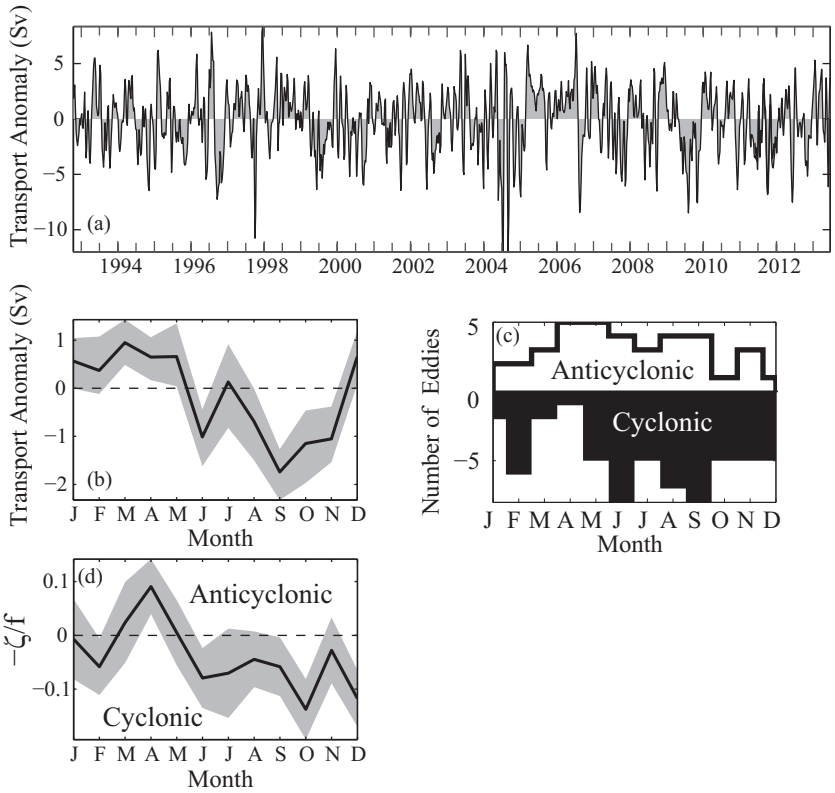

Figure 10. Analysis of 21 years of AVISO data: (a) Time series of Kuroshio transport anomaly across 18.75°N, computed using the SLA slope between 122°E and 123°E, (b) monthly variation of the Kuroshio transport anomaly, (c) total number by month of anticyclonic (positive) and cyclonic (negative) eddies within 250 km of the eastern Kuroshio boundary, and (d) monthly averaged relative vorticity of eddies.

The SLA slope between 122°E and 123°E at the mooring latitude fluctuates in unison with the observed Kuroshio transport anomalies (Figure 7c). Eight anomalous transport events >5 Sv are identified over the observation period. Kuroshio transport increases (decreases) when the SLA slope is positive (negative). The correlation between Kuroshio transport and the SLA slope is 0.9 with a 95% significance level of 0.23. A linear regression analysis suggests $\delta KT = 6 \times 10^6 (SLA\ Slope)$, where δKT is the Kuroshio transport anomaly in Sv. *Ezer* [2001] reports a good correlation between Gulf Stream transport from a numerical model with the SLA in the North Atlantic at a time scale shorter than one year. Our direct observations of Kuroshio transport are in agreement with Ezer's model results.

To distinguish whether Rossby waves or eddies are responsible for the observed Kuroshio transport changes, we use the technique by Cheng et al. (personal communication, 2014) to detect eddies arriving at the eastern limit of the Kuroshio, track eddy paths, and quantify their properties. *Nencioli et al*. [2010] develop an eddy detection method for high spatial resolution data based on vector geometry that yields a higher success rate for eddy detection than the Okubo-Weiss method [*Isern-Fontanet et al*., 2004]. Y.-H. Cheng et al. (Dynamical features of eddies interacting with the Kuroshio in east of Taiwan and the Luzon Strait, submitted to *Journal of Geophysical Research*, 2014) modify the detection method by *Nencioli et al*. [2010]. An eddy is defined as an isolated and rotational feature in a map of absolute dynamic topography (MADT). Four constraints are applied to the MADT to detect an eddy: (1) From the Okubo-Weiss method, the eddy center should be a vorticity-dominated region ($W < 0$); $W = \left(\frac{\partial v}{\partial x} + \frac{\partial u}{\partial y}\right)^2 + \left(\frac{\partial u}{\partial x} - \frac{\partial v}{\partial y}\right)^2 - \left(\frac{\partial v}{\partial x} - \frac{\partial u}{\partial y}\right)^2$. (2) The zonal gradient of the MADT has to reverse signs across the eddy center. (3) The meridional gradient of the MADT has to reverse signs across the eddy center. (4) The magnitude of the MADT at the eddy center has to be a local extreme. Once the eddy center is detected, it is tracked by identifying the closest eddy of the same polarity in the subsequent near-real time daily MADT within a radius of 75 km from the previous eddy center.

Seven eddies within 250 km of the eastern limit of the Kuroshio at the latitude of the moored array (18.75°N, 123°E) are identified (Figures 8 and 9), and tracked as far east as 130°E. Five stall and dissipate at

about 124°E. The averaged westward propagation speed |C| of these eddies is ~0.1 m s^{-1}, which is in agreement with the averaged propagation speed of eddies over the STCC reported by *Hwang et al*. [2004]. Their maximum current speed $|U_{max}|$ is typically 0.2–0.8 m s^{-1}. These eddies are nonlinear because the maximum Froude number $|U_{max}|/|C| = 2–8$. It is expected that they carry distinct water masses within their cores for a long distance [*Early et al*., 2011].

Seven anomalous Kuroshio transport events coincide with seven eddies impinging on the Kuroshio Current during the mooring observation period (Figure 9). In particular, the Kuroshio transport anomalies of more than 10 Sv in June–July 2012 (events 1 and 2) and in May to June 2013 (events 7 and 8; Figure 1) coincide with pairs of cyclonic and anticyclonic eddies. These eddies have a typical Rossby number, relative vorticity normalized by the planetary vorticity, of ~0.2. The area integrated eddy kinetic energy is of order TJ m^{-1} and the mean current speed is about 0.4 m^{-1}. Instead of westward impinging eddies, the anomalous low Kuroshio transport event in April 2013 (labeled "6" in Figure 7c) appears to be modulated by a high SLA event to the west of 122°E in Luzon Strait (Figure 7a). A close examination of this high SLA event indicates that it is due to an eddy-like process that is generated locally in Luzon Strait west of the Kuroshio.

4. Seasonal Variation of Kuroshio Transport

The result of linear regression analysis performed on the local SLA slope and the observed Kuroshio transport anomaly δKT at the entrance to Luzon Strait (section 3), $\delta KT = 6\ x\ 10^6(SLA\ \ Slope)$, is applied to SLA data from the period 1992 to 2013 (Figure 10). The inferred Kuroshio transport anomaly varies between −12 Sv and 7 Sv, with a standard deviation of 3 Sv. Spectral analysis shows a significant peak at a 1 year period (not shown). Monthly averages reveal a seasonal cycle, with stronger (weaker) Kuroshio transport in winter and spring (summer and fall) (Figure 10b). The interannual variation of the Kuroshio transport anomaly is removed using a high-pass filter to remove variance greater than 500 days. The amplitude of seasonal variation is ~1 Sv.

Identification of eddies within 250 km of the eastern Kuroshio boundary at the mooring latitude during 1992–2013 yields a total of 34 anticyclonic and 60 cyclonic eddies. More anticyclonic eddies impinge on the Kuroshio boundary in spring than in other seasons and more cyclonic eddies in summer and fall (Figure 10c). *Hwang et al*. [2004] report that more anticylonic eddies in summer and more cyclonic eddies in winter averaged in the entire STCC zone. We cannot compare our results with those of *Hwang et al*. [2004] because the time taken for eddies to arrive at the Kuroshio from the STCC zone depends on their generation location and propagation speed.

Monthly averaged eddies' relative vorticity is strongest anticyclonic in spring and strongest cyclonic in fall. Our analysis shows stronger Kuroshio transport, more anticyclonic eddies impinging on the eastern limit of the Kuroshio, and strongest anticylonic vorticity in spring. In fall, the Kuroshio transport is weak and cyclonic eddies prevail. Because anticyclonic (cyclonic) eddies can enhance (suppress) Kuroshio transport, our results suggest that the seasonal cycle of Kuroshio transport at this location can be explained partially by the impinging eddies.

Qiu and Lukas [1996] report a similar seasonal cycle from a wind-driven numerical model simulation and attribute it to the seasonal migration of the NEC bifurcation latitude; specifically, the Kuroshio transport off Luzon decreases (increases) when the NEC bifurcation shifts northward (southward). Their model, however, fails to simulate the STCC and therefore does not capture the mesoscale eddies along the 18°N−25°N band. *Yaremchuk and Qu* [2004] report a similar seasonal variation. These two studies report seasonal variations of 3–5 Sv, larger than our observations, but all three show strong (weak) Kuroshio transport in spring (fall). Differences in amplitude may be due to no simulated eddies or model inaccuracies in *Qiu and Lukas* [1996], an inappropriate choice of the level of no motion in *Yaremchuk and Qu* [2004], or this study's errors in the estimation of Kuroshio transport anomaly.

5. Summary

Direct velocity observations of the Kuroshio at its entrance to Luzon Strait show an annual mean transport of 15 Sv with strong temporal variations (Figure 7). The position of the Kuroshio axis remains extremely stable over the 1 year observation period. The relative vorticity is much smaller than the planetary vorticity,

except in the upper 150 m west of the Kuroshio axis. Therefore, the Kuroshio is in approximate geostrophic balance. The Kuroshio transport is strongly correlated with the SLA slope across the moored array. Eight anomalous transport events are identified over the 1 year record of observations. Kuroshio transport anomalies of $>$10 Sv in O(10) days result from impinging pairs of cyclonic and anticyclonic eddies. Of the eight observed anomalous events, seven are due to westward propagating nonlinear eddies (Figure 9). One is due to a high SLA event inside Luzon Strait. The long-term SLA slope data from altimeter measurements are analyzed as a proxy for the Kuroshio transport anomalies. Kuroshio transport is maximum (minimum) in spring (fall) (Figure 10). Analysis of eddies shows anticyclonic vorticity prevails in spring and cyclonic vorticity in fall. We speculate that the seasonal cycle of the Kuroshio transport may be modulated both by the westward propagating eddies and the wind-driven migration of the NEC bifurcation latitude as suggested by *Qiu and Lukas* [1996]. These two processes are potentially coupled. Long-term Kuroshio transport measurements are needed to confirm the derived seasonal variation. The mesoscale eddies detected in our analysis are nonlinear, with their particle speed exceeding propagation speed. Originating along the baroclinically unstable STCC, these westward propagating eddies likely carry interior ocean water masses and, when impinging upon the Kuroshio, have the potential to alter Kuroshio water properties. Further investigation of the eddy-Kuroshio interactions is needed to understand the processes and to better predict Kuroshio variability and its impact on marginal seas' circulation.

Acknowledgments

The authors appreciate all the constructive comments from reviewers. We thank V. Sheremet and J. Kuehl for sharing their expertise and for providing the Matlab program to solve the QG equation. We also thank T. Sanford from the Applied Physics Laboratory of the University of Washington, the R/V *Revelle* crew and officers, W.-H. Her and V. Mensah from National Taiwan University, and Philippine colleagues for their help deploying and recovering moorings. We also greatly appreciate S. Jan and Y. J. Yang from National Taiwan University for coordinating the experiment. The altimeter products used in this analysis were produced by Ssalto/Duacs and distributed by Aviso, with support from CNES (http://www.aviso.oceanobs.com/duacs/). Lien, Ma, Qiu, and Lee were supported by the Office of Naval Research Departmental Research Initiative *Origins of the Kuroshio and Mindanao Currents* grants N00014-10-1-0397 (Lien and Ma), N00014-10-1-0267 (Qiu), and N00014-10-1-0308 (Lee).

References

Barron, C. N., A. B. Kara, and G. A. Jacobs (2009), Objective estimates of westward Rossby wave and eddy propagation from sea surface height analysis, *J. Geophys. Res.*, *114*, C03013, doi:10.1029/2008JC005044.

Centurioni, L. R., P. P. Niiler, and D.-K. Lee (2004), Observations of inflow of Philippine Sea water into the South China Sea through the Luzon Strait, *J. Phys. Oceanogr.*, *34*, 113–121.

Chang, M.-H., T. Y. Tang, C. R. Ho, and S.-Y. Chao (2013), Kuroshio-induced wake in the lee of Green Island off Taiwan, *J. Geophys. Res. Oceans*, *118*, 1508–1519, doi:10.1002/jgrc.20151.

Chang, Y.-L., and L.-Y. Oey (2012), The Philippines–Taiwan oscillation: Monsoonlike interannual oscillation of the subtropical-tropical western north Pacific wind system and its impact on the ocean, *J. Clim.*, *25*, 1597–1618, doi:10.1175/JCLI-D-11-00158.1.

Chelton, D. B., M. G. Schlax, R. M. Samelson, and R. A. de Szoeke (2007), Global observations of large oceanic eddies, *Geophys. Res. Lett.*, *34*, L15606, doi:10.1029/2007GL030812.

Chelton, D. B., M. G. Schlax, and R. M. Samelson (2011), Global observations of nonlinear mesoscale eddies, *Prog. Oceanogr.*, *91*, 167–216.

Early, J. J., R. M. Samelson, and D. B. Chelton (2011), The evolution and propagation of quasigeostrophic ocean eddies, *J. Phys. Oceanogr.*, *41*, 1535−1555.

Eriksen, C. C., T. J. Osse, R. D. Light, T. Wen, T. W. Lehman, P. L. Sabin, J. W. Ballard, and A. M. Chiodi (2001), Seaglider: A long-range autonomous underwater vehicle for oceanographic research, *IEEE J. Oceanic Eng.*, *26*(4), 424–436.

Ezer, T. (2001), Can long-term variability in the Gulf Stream transport be inferred from sea level? *Geophys. Res. Lett.*, *28*, 1031–1034.

Gilson, J., and D. Roemmich (2002), Mean and temporal variability in Kuroshio geostrophic transport south of Taiwan (1993–2001), *J. Oceanogr.*, *58*, 183–195.

Hsin, Y.-C., B. Qiu, T.-L. Chiang, and C.-R. Wu (2013), Seasonal to interannual variations in the intensity and central position of the surface Kuroshio east of Taiwan, *J. Geophys. Res. Oceans*, *118*, 4305–4316, doi:10.1002/jgrc.20323.

Hwang, C., C.-R. Wu, and R. Kao (2004), TOPEX/Poseidon observations of mesoscale eddies over the STCC, *J. Geophys. Res.*, *109*, C08013, doi:10.1029/2003JC002026.

Isern-Fontanet, J., J. Font, E. Garcia-Ladona, M. Emelianov, C. Millot, and I. Tauper-Letage (2004), Spatial structure of anticyclonic eddies in the Algerian basin (Mediterranean Sea) analyzed using the Okubo-Weiss parameter, *Deep Sea Res., Part I*, *51*, 3009–3028.

Jan, S., R.-C. Lien, and C.-H. Ting (2008), Numerical study of baroclinic tides in Luzon Strait, *J. Oceanogr.*, *64*, 789–802.

Johns, W. E., D. R. Watts, and H. T. Rossby (1989), A test of geostrophy in the Gulf Stream, *J. Geophys. Res.*, *94*, 3211–3222.

Johns, W. E., T. N. Lee, D. Zhang, R. Zangtopp, C. T. Liu, and Y. Yang (2001), The Kuroshio east of Taiwan: Moored transport observations from the WOCE PCM-1 array, *J. Phys. Oceanogr.*, *31*, 1031–1053.

Kobashi, F., and H. Kawamura (2002), Seasonal variation and instability nature of the North Pacific Subtropical Countercurrent and the Hawaiian Lee Countercurrent, *J. Geophys. Res.*, *107*(C11), 3185, doi:10.1029/2001JC001225.

Kontoyiannis, H., and D. R. Watts (1990), Ageostrophy and pressure work in the Gulf Stream at 73°W. *J. Geophys. Res.*, *95*, 22,209–22,228.

Kuehl, J., and V. A. Sheremet (2009), Identification of a cusp catastrophe in a gap-leaping western boundary current, *J. Mar. Res.*, *67*(1), 25–42.

Lee, I.-H., D. S. Ko, Y.-H. Wang, L. Centurioni, and D.-P. Wang (2013), The mesoscale eddies and Kuroshio transport in the western North Pacific east of Taiwan from 8-year (2003–2010) model reanalysis, *Ocean Dyn.*, *63*, 1027–1040, doi:10.1007/s102360-0012-0643-z.

Liang, W.-D., T. Y. Tang, Y. J. Wang, M. T. Ko, and W.-S. Chuang (2003), Upper-ocean currents around Taiwan, *Deep Sea Res., Part II*, *50*, 1085–1105.

Munk, W. H. (1950), On the wind-driven ocean circulation, *J. Meteorol.*, *7*, 79–93.

Nencioli, F., C. M. Dong, T. Dickey, L. Washburn, and J. C. McWilliams (2010), A vector geometry-based eddy detection algorithm and its application to a high-resolution numerical model product and high-frequency radar surface velocities in the southern California bight, *J. Atmos. Oceanic Technol.*, *27*, 564–579.

Nitani, H. (1972), Beginning of the Kuroshio, in *Kuroshio: Its Physical Aspects*, edited by H. Stommel and K. Yoshida, pp. 129–163, Univ. of Tokyo Press, Tokyo.

Qiu, B. (1999), Seasonal eddy field modulation of the North Pacific subtropical countercurrent: TOPEX/POSEIDON observations and theory, *J. Phys. Oceanogr.*, *29*, 2471–2486.

Qiu, B. (2002), The Kuroshio extension system: Its large-scale variability and role in the midlatitude ocean-atmosphere interaction. *J. Oceanogr.*, *58*, 57–75.
Qiu, B., and R. Lukas (1996), Seasonal and interannual variability of the North Equatorial Current, the Mindanao Current and the Kuroshio along the Pacific western boundary, *J. Geophys. Res.*, *101*, 12,315–12,330.
Qu, T., H. Mitsudera, and T. Yamagata (1998), On the western boundary currents in the Philippine Sea, *J. Geophys. Res.*, *103*, 7537–7548.
Ratsimandresey, A. W., and J. L. Pelegri (2005), Vertical alignment of the Gulf Stream, *Tellus, Ser. A*, *57A*, 691–700.
Rhodes, R. C., et al. (2002), Navy real-time global modeling systems, *Oceanography*, *15*(1), 29−43, doi:10.5670/oceanog.2002.34.
Roemmich, D., and J. Gilson (2001), Eddy transport of heat and thermocline waters in the North Pacific: A key to interannual/decadal climate variability? *J. Phys. Oceanogr.*, *31*, 675–687.
Sheremet, V. (2001), Hysteresis of western boundary current leaping across a gap, *J. Phys. Oceanogr.*, *31*, 1247–1259.
Sheremet, V. A., G. R. Ierley, and V. M. Kamenkovich (1997), Eigenanalysis of the two-dimensional wind-driven ocean circulation problem, *J. Mar. Res.*, *55*, 57−92.
Sverdrup, H. U. (1942), *Oceanography for Meteorologists*, 246 pp., Prentice Hall, New York.
Toole, J. M., R. C. Millard, Z. Wang, and S. Pu (1990), Observations of the Pacific North Equatorial Current bifurcation at the Philippine coast, *J. Phys. Oceanogr.*, *20*, 307–318.
Vélez-Belchí, P., L. R. Centurioni, D. K. Lee, S. Jan, and P. P. Niiler (2013), Eddy induced Kuroshio intrusions onto the continental shelf of the East China Sea, *J. Mar. Res., 71*, 83–108.
Wyrtki, K. (1961), *Physical Oceanography of the Southeast Asian Waters, NAGA Report 2*, 195 pp., Scripps Inst. of Oceanogr., Univ. of Calif. San Diego, La Jolla, Calif.
Yang, Y., C.-T. Liu, J.-H. Hu, and M. Koga (1999), Taiwan Current (Kuroshio) and impinging eddies, *J. Oceanogr.*, *55*, 609–617.
Yaremchuk, M., and T. Qu (2004), Seasonal variability of the large-scale currents near the coast of Philippines, *J. Phys. Oceanogr.*, *34*(4), 844–855.
Zhang, D. T., T. N. Lee, W. E. Johns, C.-T. Liu, and R. Zantopp (2001), The Kuroshio east of Taiwan: Modes of variability and relationship to interior ocean mesoscale eddies, *J. Phys. Oceanogr.*, *31*, 1054–1074.